Penerbit Akademia Baru

Journal of Advanced Research in Fluid Mechanics and Thermal Sciences
ISSN (online): 2289-7879 | Vol. 4, No. 1. Pages 23-35, 2014

The Effects of Row Trench Holes with Alignment Angle of +60 Degrees on Film Cooling Effectiveness at Low Blowing Ratios

E. Kianpour [*,1,a] *and I. Golshokouh* [2]

[1]Faculty of Engineering, Islamic Azad University of Najaf Abad, Esfahan, Iran
[2]Faculty of Mechanical Engineering, Islamic Azad University of Izeh, Khuzestan, Iran
[*]*ekianpour@gmail.com*

Abstract – *This study was accomplished to study the effects of cylindrical and row trenched cooling holes with alignment angle of +60 degrees at low blowing ratio, BR = 1.25 on the film cooling effectiveness near the combustor end wall surface. In this research, a three-dimensional representation of a Pratt and Whitney gas turbine engine was simulated and analyzed with a commercial finite volume package FLUENT 6.2.26. The current study has been performed with Reynolds-averaged Navier-Stokes turbulence model (RANS) on internal cooling passages. This combustor simulator combined the interaction of two rows of dilution jets that were staggered in the stream wise direction and aligned in the span wise direction, with that of film cooling along the combustor liner walls. The findings of the study declared that by using the row trenched holes near the end wall surface, film cooling effectiveness is doubled compared to the cooling performance of baseline case.*

Keywords: Gas Turbine, Film Cooling, Trenched Holes, Shaped Holes, Compound Holes

1.0 INTRODUCTION

Gas turbine industries strive for higher engine efficiencies. Brayton cycle is a key to this study. According to this cycle, the turbine inlet temperature should increase to gain more efficiency. However, increasing the turbine inlet temperature creates an extremely harsh environment for critical downstream components. Therefore, there is a need to design a cooling technique in this area. Film cooling is a traditional way in which it is used. In this system, a thin thermal boundary layer is formed by cooling holes and attached on the protected surface. Cylindrical and trenched cooling holes are two layouts of these holes.

Researchers have studied the effect of various cooling hole geometries for film cooling performance. Vakil and Thole [1] and Barringer *et al*. [2] presented the experimental results of the combustor simulator. They applied a real scale combustor, and the coolant flow and high momentum of dilution jets were injected into the main flow. They found that a high temperature gradient was developed upstream of the dilution holes. In addition, the results indicated that the dilution jets reduced the total pressure and velocity fields, and the turbulence level at the end of the combustor reached 24%. This quantity is a little bit lower compared to Colban *et al*.'s [3] findings, which predicted the turbulence level between 25% and 30%. Kianpour *et al*. [4, 5] simulated the same model using k-ε and RNG k-ε turbulent models to solve the Navier-Stokes equation. They claimed that the RNG k-ε turbulent model was a good choice to detect

the variation of temperature in the combustor simulator. This finding was later confirmed by Colban et al. [3], Patil *et al*. [6], and Scheepers and Morris [7]. They demonstrated the consistency of the results between experimental and numerical approaches by using the RNG k-ε turbulent model. In another study, Sundaram and Thole [8] and Baheri *et al*. [9] investigated the effects of modified trench depth in order to increase the film cooling effectiveness. The study was conducted with various individual and row trench depths. They reported that the maximum cooling effectiveness can be obtained when the trench depth was d = 0.8D (d is the trench depth and D is the diameter of the cooling hole). However, Lawson and Thole [10] found different results, suggesting that this trench depth gives a negative effect on the cooling performance downstream the cooling hole. Later, Lu *et al.* [11] and Maikell et al. [12] found that the trench depth of d=0.75D gave the optimum efficiency and it was validated by CFD studies. In another study, Barigozzi *et al*. [13] suggested that high efficiency can be obtained when d/D = 1.0 but it is restricted to low blowing ratio condition.

The effect of blowing ratio on the film cooling efficiency has also attracted few studies. Somawardhana and Bogard [14] investigated the effects of shallow trenched holes on the turbine vane cascade in the presence of obstructions. The adiabatic effectiveness was calculated for blowing ratios from 0.4 to 1.6. The results indicated that while upstream obstructions reduced the effectiveness by 50%, the downstream obstructions increased the performance of film cooling for all blowing ratios. Furthermore, a combination of both obstructions slightly affected the performance of film cooling and the results were close to the case of upstream obstructions. They also concluded that the adiabatic effectiveness with the narrow trench was relatively constant across this range of blowing ratios. However, these results were inconsistent with Harrison *et al*. [15], Shuping [16], Baheri Islami and Jurban [17], and Lu and Ekkad [18], which stated that when the blowing ratio increased from 0.6 to 1.4, the performance of the trench was three times greater than that for baseline cylindrical holes. Recently, Ai *et al*. [19] proved that trenching reduced the coolant momentum ratio and impaired the effectiveness while traditional cooling holes performance was better at low blowing ratios.

The study on film cooling efficiency using fan-shaped cooling was performed by Colban *et al*. [20, 21] for blowing ratios from 2.8 to 8.5. They reported that for a constant blowing ratio, the fan-shaped holes increased film cooling effectiveness by an average of 75% over cylindrical holes. The above finding was consistent with the study by Peng and Jiang [22]. Peng and Jiang examined the effect of blowing ratio in the range of 0.5 to 1.5 on the film cooling effectiveness using fan-shaped cooling holes. They concluded that the film cooling performance increased as the blowing ratio increased, which differs from that of the cylindrical hole. For the case of fan-shaped hole model, as the blowing ratio increased, the cooling gas flow rate increased; hence, there is more cooling gas to protect the wall, and the film cooling effectiveness increased. In addition, according to Lutum *et al*. [23] and Gao *et al*. [24], higher film cooling performance was observed for the fan-shaped holes at higher blowing ratios compared to cylindrical cases.

It appears from the aforementioned investigations that numerous investigations have been conducted on the effects of internal cooling holes. However, no attempt has been made to investigate the effects of trenching of the cooling holes near the combustor end wall surface on the film cooling effectiveness. The primary zone that senses this high temperature gas is the combustor end wall surface. Developing more effective cooling that covers the area adjacent to the wall is important because without this layer, the outlet combustion temperature increment is not reasonable. It threatens the life of the end wall surface of the combustor and imposes high costing services to the customers. Furthermore, the improvement of film cooling layer

adjacent to the combustor end wall surface assists the designers to make better operable condition for the engine, as well as increasing the efficiency. Therefore, the objective of the present study was to investigate the change of film cooling effectiveness with different arrangements of cooling holes as the baseline case and trenched holes at different blowing ratios.

2.0 RESEARCH METHODOLOGY

In this study, a three-dimensional representation of a true Pratt and Whitney engine was simulated and analyzed to gain essential data. The schematic view of the combustor is shown in Fig. 1. The width and inlet height of the final combustor simulator design were 111.8 cm and 99.1 cm, respectively. The length of the combustor was 156.9 cm and the contraction angle was 15.8 degrees. The contraction angle began at x = 79.8 cm. The inlet cross-sectional area was 1.11 m^2 and the exit cross-sectional area was reduced to 0.62 m^2. The combustor simulator included four film-cooled stream wise panels. The starting point of these panels was approximately at 1.6 m upstream of the turbine vanes. The first and second panels were 39.2 and 40.6 cm in length, respectively. The length of the next two panels was 36.8 cm and 43.2 cm. The low thermal conductivity of combustor panels was 1.27 cm in thickness, which allowed for adiabatic surface temperature measurements. Two different rows of dilution holes were considered within the second and third panels. These dilution rows were located at 0.67 m and 0.90 m downstream of the beginning of the combustor liner panels. The diameter of the dilution holes at the first and second rows was 8.5 cm and 11.9 cm, respectively.

The center line of the second row was staggered with respect to the first row of dilution holes. To verify the purpose of this study, a three-dimensional representation of a Pratt and Whitney gas turbine engine was simulated. The present combustor simulator included two configurations of cooling holes. The first arrangement (baseline) was designed similar to Vakil and Thole [1]. In both cases, the film cooling holes were placed in equilateral triangles. The diameter of the film cooling holes was 0.76 cm and drilled at an angle of 30 degrees from the horizontal surface. The length of film cooling holes in the baseline case was 2.5 cm. For the second case (Case 2), the cooling holes were embedded within a row trenched with alignment angle of +60 degrees, as shown in (Fig. 2). Furthermore, the trench depth and width were 0.75D and 1.0D, respectively.

The purpose of this study was to investigate the effects of cooling holes structure on the film cooling effectiveness within a combustor simulator at different coolant blowing ratios. In comparing the results, a number of non-dimensional parameters need to be defined. The dimensionless variables were defined for both the coolant and dilution flow. Table 1 gives a complete description of the operating conditions for the main flow, while Table 2 shows the non-dimensional parameters of the dilution jets and coolant, respectively.

Penerbit Akademia Baru
Journal of Advanced Research in Fluid Mechanics and Thermal Sciences
ISSN (online): 2289-7879 | Vol. 4, No. 1. Pages 23-35, 2014

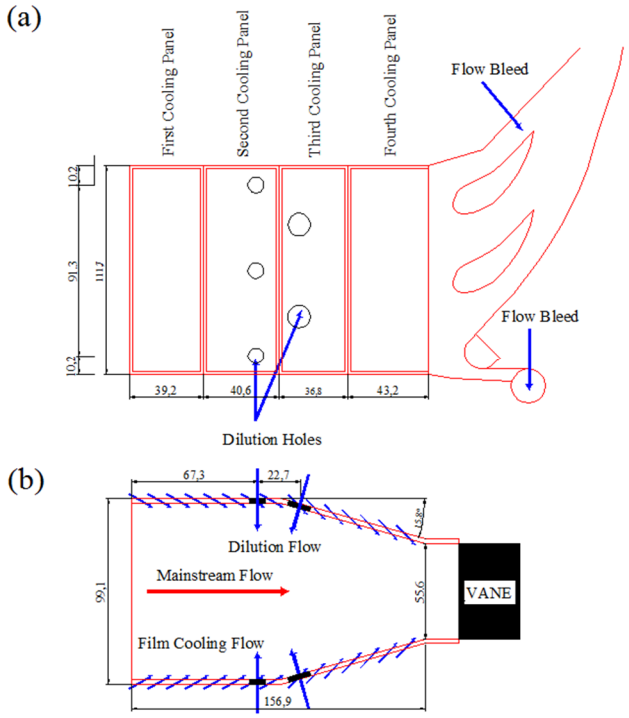

Figure 1: Schematic of the combustor simulator (a) top view and (b) side view (all dimensions are in cm)

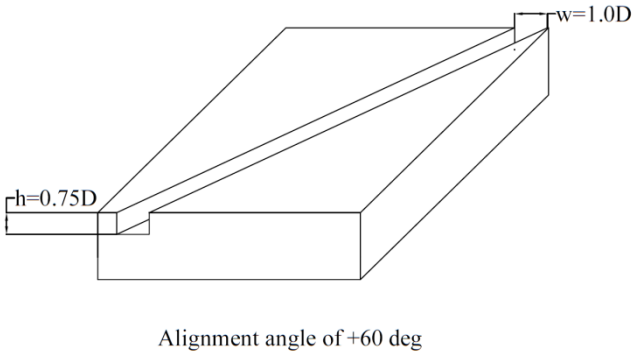

Figure 2: Schematic geometry of row trenched cooling holes with alignment angle of +60 degrees

Also, the temperature of the coolant and dilution jets was considered equal to 295.5K. The thermal distribution inside a combustor simulator was measured along the specific measurement planes. These measurement planes are shown in (Fig. 3). In order to get more accurate data and reasonable time consumption, about 8 × 106 tetrahedral meshes were used as adopted in the study by Stitzel and Thole [25].

According to the specific flow ratio at the inlet of volume control, inlet mass flow boundary condition was defined. Wall boundary condition and slipless boundary condition were applied to limit the interaction zone between fluid and solid layer. The pressure outlet boundary

Penerbit Akademia Baru
Journal of Advanced Research in Fluid Mechanics and Thermal Sciences
ISSN (online): 2289-7879 | Vol. 4, No. 1. Pages 23-35, 2014

condition was used at the end of volume control. In addition, both cases were completely symmetrical along the x-y and x-z planes.

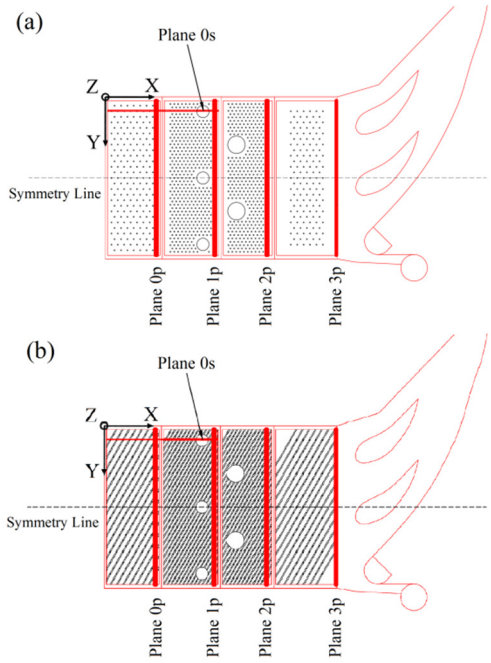

Figure 3: Location of the measurement planes (a) baseline and (b) Case 2

According to this issue, symmetry boundary condition $\partial/(\partial n=0)$ was as applied. In addition, the following equations were used as well. The governing equations for the current case study are:

Momentum equation:

$$\frac{\partial}{\partial t}(\rho u_i)+\frac{\partial}{\partial x_j}=(\rho u_i u_j)=-\frac{\partial P}{\partial x_i}+\frac{\partial \tau_{ij}}{\partial x_i}+\rho g_i+\overrightarrow{F_i} \quad (1)$$

Continuity equation:

$$\frac{\partial \rho}{\partial t}+\frac{\partial}{\partial x}\frac{dx}{dt}+\frac{\partial \rho}{\partial y}\frac{dy}{dt}+\frac{\partial \rho}{\partial z}\frac{dz}{dt}=-\rho(\nabla.V) \quad (2)$$

Energy and RNG k-ε equations:

$$\frac{\partial}{\partial t}(\rho k)+\frac{\partial}{\partial x_i}(\rho k u_i)=\frac{\partial}{\partial x_j}\left[\left(\mu+\frac{\mu_t}{\sigma_k}\right)\frac{\partial k}{\partial x_j}\right]+P_k-\rho\grave{o} \quad (3)$$

$$\frac{\partial}{\partial t}(\rho\grave{o})+\frac{\partial}{\partial x_i}(\rho\grave{o}u_i)=\frac{\partial}{\partial x_j}\left[\left(\mu+\frac{\mu_t}{\sigma_{\grave{o}}}\right)\frac{\partial\grave{o}}{\partial x_j}\right]+C_{1\grave{o}}\frac{\grave{o}}{k}P_k-C^*_{2\grave{o}}\rho\frac{\grave{o}^2}{k} \quad (4)$$

Penerbit Akademia Baru
Journal of Advanced Research in Fluid Mechanics and Thermal Sciences
ISSN (online): 2289-7879 | Vol. 4, No. 1. Pages 23-35, 2014

The first-order upwind and central differencing scheme were used to approximate the convective and diffusion terms in the differential equation, respectively. To check the convergence, the mass residue of each control volume has been calculated and the maximum value has been used to check for the convergence. The convergence criterion has been set to 10^{-4}. To understand the thermal field results, the quantities should be defined. Film cooling effectiveness is defined as below:

$$\eta = \frac{T - T_\infty}{T_C - T_\infty} \tag{5}$$

In the equation above, T is the local temperature, T_∞ is the main stream temperature, and T_C is the temperature of coolant.

3.0 RESULTS AND DISCUSSION

Comparisons have been made for the baseline case using the experimental results by Vakil and Thole [1], computational results by Stitzel and Thole [25], and the current study. The model used in this computational study was the RNG k-ε model. The biggest difference between the standard and RNG models is the addition of the R term in the transport equation for turbulence dissipation. This term makes the RNG model more responsive to the effects of rapid strain and streamlines curvature, thus improving the model, particularly for separated flows, recirculating flows and end wall secondary flows. Fig. 4 presents the comparison of film cooling effectiveness for plane 1p and 2p at y/W = 0.4. The deviations between the current computation and benchmarks were calculated as follows:

$$\%Diff = \frac{\sum_{i=1}^{n} \frac{x_i - x_{i,benchmark}}{x_{i,benchmark}}}{n} \times 100 \tag{6}$$

According to this formula, the deviation was equal to 9.76% and 8.34% compared to [1, 25] for plane 1p and equal to 13.36% and 11.96% compared to [1, 25] for plane 2p.

Fig. 5 shows the results of the thermal field predictions made for plane 0p at low blowing ratio of BR=1.25. Recall that η was defined as the difference in the free stream and the local measured temperature divided by the difference in the free stream and coolant temperature (equation 6). The observation plane was located at x/L = 0.24, which was two film-cooling hole diameters (2d) downstream of the trailing edge of the last row of the cooling holes in panel one. Since the liner panels were made to represent a staggered film-cooling pattern, the dashed arrows denote the upstream film-cooling holes, whereas the solid arrows show the downstream holes. There was a total of 15 rows of staggered film-cooling holes present in panel 1 with the hole spacing.

Penerbit Akademia Baru
Journal of Advanced Research in Fluid Mechanics and Thermal Sciences
ISSN (online): 2289-7879 | Vol. 4, No. 1. Pages 23-35, 2014

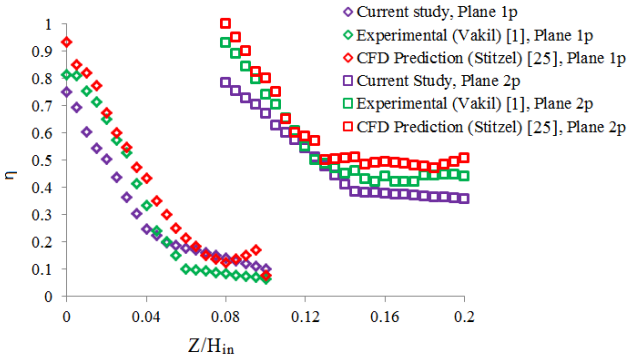

Figure 4: The comparison of film cooling effectiveness for plane 1p and 2p along y/W=0.4

The jets closest to the observation plane (the last row on panel 1) had their coolest region near the wall with a secondary cool region directly above it. This secondary cool region was a remnant of the upstream film-cooling jet that exited from the aligned cooling hole. This effect was negligible in the upstream holes because the two regions were combined in this location. Also, it appeared that in this location, the core of the jets from the upstream row was further away from the wall of the downstream row. We suggest producing a cold protected layer near the end wall surface that can be made possible by using a trenched hole. However, hotter region (0< <0.05) was seen in a further distance from the end wall surface (5 cm<z<10 cm), particularly in the case of the configurations of trenched holes with an alignment angle of +60 degrees.

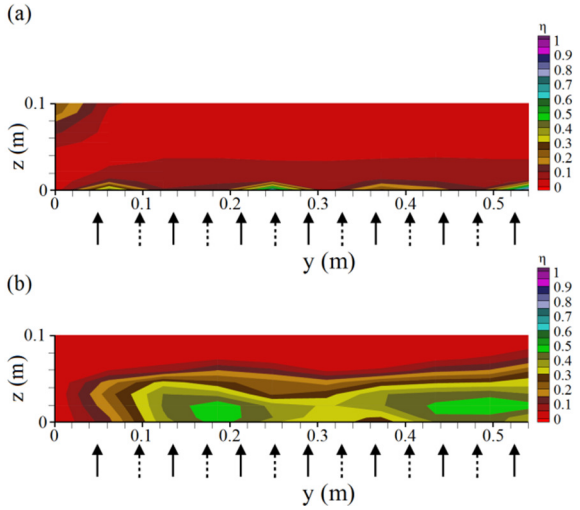

Figure 5: Film-cooling effectiveness distribution of plane 0p for (a) baseline case and (b) Case 2

Film cooling effectiveness in plane 1p was taken directly downstream of the first row of the dilution jets. This particular hole is centrally located right at the mid pitch within the combustor simulator. The results of the thermal field are shown in Fig. 6. Plane 1p approximately extended from y/W=0 to y/W=0.50 in the pitch wise direction, therefore it covered one-half of a sector. As Fig.6 illustrates, the center of the dilution jet is reasonably centered about the corners of this observation plane as the dilution jet surges up. Note that jet spreading there is slightly higher for y=10 cm and y=50 cm. This may be due to the jet's interaction with its top row. Also, contrary to the baseline, it is slightly hotter (0<η<0.05) for the trenched case with the

Penerbit Akademia Baru
Journal of Advanced Research in Fluid Mechanics and Thermal Sciences
ISSN (online): 2289-7879 | Vol. 4, No. 1. Pages 23-35, 2014

alignment angle of +60 degrees in the position of 14 cm<y<52 cm and 8 cm<z<10 cm. However, compared to other cases, this type of trenched holes, adjacent to end wall surfaces, perform more efficiently. In general, the measurements indicate the existence of proper symmetry across the pitch of the combustor simulator. The existence of symmetry in the thermal fields implies its existence within the velocity flow fields. In fact, thermal fields are quite sensitive to variations in velocity. Obscurities in thermal results serve as an obvious indication of variations in velocity across the pitch or the span.

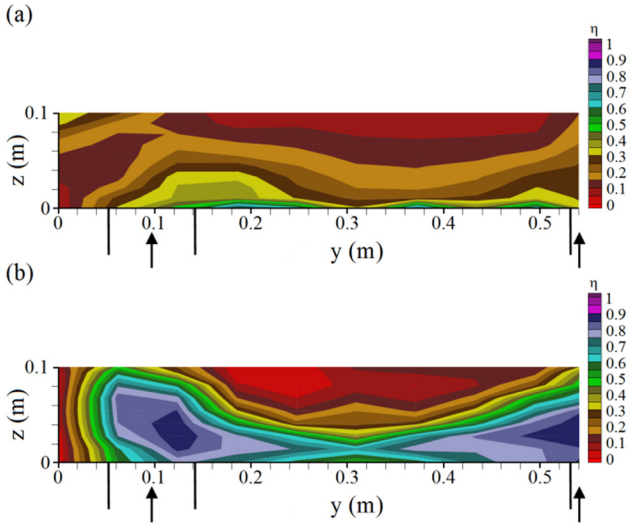

Figure 6: Film-cooling effectiveness distribution of plane 1p for (a) baseline case and (b) Case 2

Fig. 7 shows the contours of film cooling effectiveness in plane 2p at BR=1.25 located one dilution hole diameter (1D2) downstream of the trailing edge of a dilution two hole. The plane covers almost half pitch of the combustor simulator and shows the second rows of dilution in reasonable detail. As can be seen on the right of the figure, the mushroom shaped temperature profiles got mixed and a warmer region near the mid-span emerged. There is a probability that the warm region is formed as a result of the flow of unmixed warmer fluid around the stagnation region caused by the impact of opposing dilution jets in the first row. The high temperature region observed along y=52 cm and height of z=15 cm was the footprint of the warm fluid trapped in the recirculating region downstream of the first row of dilution jets. This region was warmer for the trenched holes row with the alignment angle +60 degrees (0<η<0.05). The thermal contours of the second row of dilution are visible on the left of Fig. 7. Absolutely visible, however, is the lack of uniformity within the combustor exiting profile at this point. At the midspan, the remnants of trapped fluid behind the first row dilution jet show core temperatures ranging between 0<η< 0.05 for the row trenched cooling holes with the alignment angle +60 degrees. The second row dilution jet's core is almost twice as cold with the values between 0.5<η<0.55 located 6 cm<y<12 cm and 18 cm<z<22 cm. With only 31% of the combustor's length left and no more rows of dilution, a streaky, non-uniform temperature profile at the combustor exit is highly likely. A non-uniform temperature field, which implies a lack of proper mixing, is clearly undesirable for a number of reasons including burnouts on the turning vanes and the unburned fuel exiting the combustor. In this figure, the dashed arrows denote the upstream dilution jets, whereas the solid arrows show the downstream jets.

Penerbit Akademia Baru
Journal of Advanced Research in Fluid Mechanics and Thermal Sciences
ISSN (online): 2289-7879 | Vol. 4, No. 1. Pages 23-35, 2014

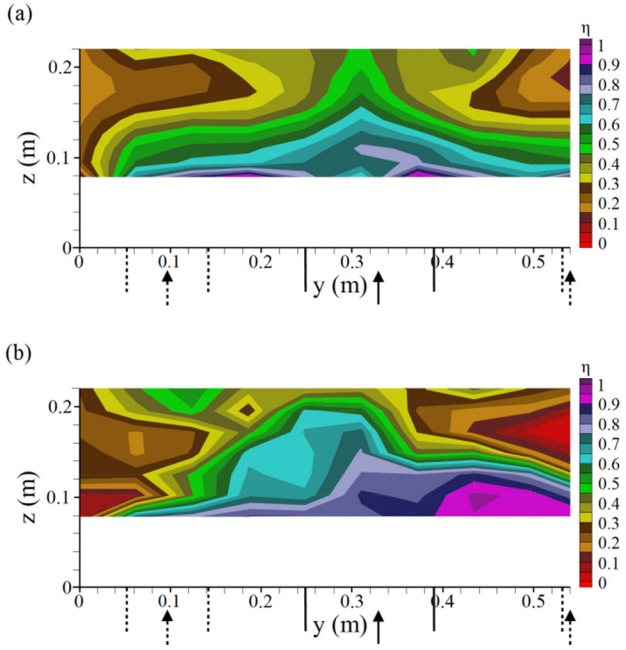

Figure 7: Film-cooling effectiveness distribution of plane 2p for (a) baseline case and (b) Case 2

Fig. 8a-e shows the film cooling effectiveness distribution for plane 3p and illustrates the behavior of the flow at the end of the combustor simulator where x/L is equal to 1.0. The largest fluctuations in the stream-wise temperature were found near 32 cm<z<38 cm for the trenched holes with the alignment angle +60 degrees. For these two types of row trenched cooling holes, the mushroom shaped temperature profiles have mixed together and a warmer region on the corners has emerged. This warm result from the unmixed warmer flowing around the stagnation region that was created by the dilution jets interaction in the second row. The stream wise jet temperature component indicated the existence of a laminar flow at the end of the combustor. A secondary cool region is seen directly above the contours (0 cm<y<16 cm) and (50 cm<y<54 cm), which is a remnant of the upstream dilution jet in the first row. This secondary cool region is severe for the trenched cooling holes with the alignment angle +60 degrees. At the midspan, the remnants of trapped fluid downstream the second row dilution jet show core temperature ranging between $0.45<\eta<0.65$.

4.0 CONCLUSION AND RECOMMENDATION

The objective of this study was to analyze the effects of using row trenched cooling holes with the alignment angle of +60 degrees on film cooling effectiveness at low blowing ratio of BR=1.25 at the end of the combustor simulator. In this study, a three-dimensional representation of a Pratt and Whitney engine was simulated and analyzed. To sum up, the application of trenched cooling holes significantly developed the film cooling layer. Also, the corners of the plane 1p showed the intense penetration of the coolant and a thick film cooling layer creation in the trenched cases. Initially, the results showed that trenched cooling holes have an intense effect on film cooling effectiveness. Comparison between experimental and computational results shows that the prediction of the film cooling exhibited a thinner film cooling layer for the current study.

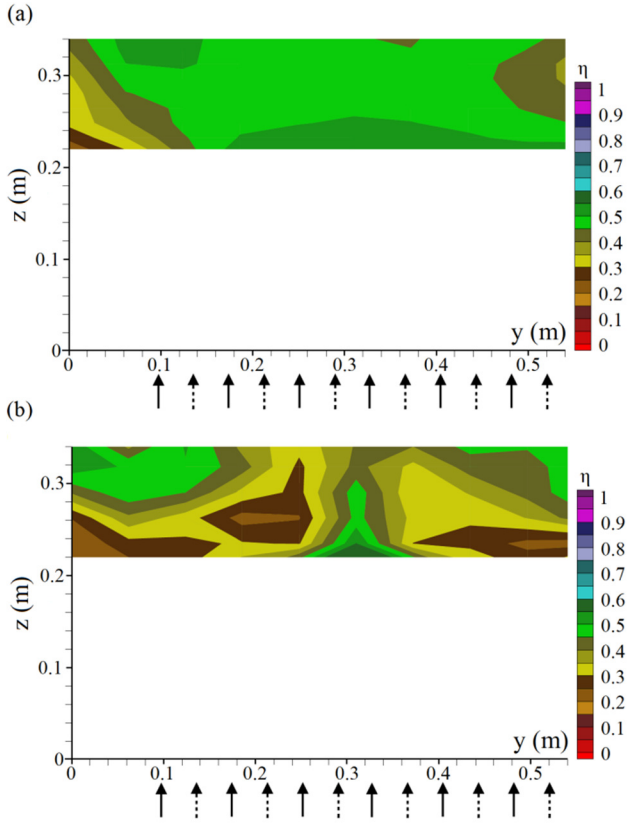

Figure 8: Film-cooling effectiveness distribution of plane 3p for (a) baseline case and (b) Case 2

Based on the results and conclusions of the study, for future research within this area, different configurations of trenched cooling holes and baseline case should be considered for different cooling panels.

REFERENCES

[1] S.S. Vakil, K.A. Thole, Flow and thermal field measurements in a combustor simulator relevant to a gas turbine aeroengine, Journal of Engineering for Gas Turbines and Power 127 (2005) 257-267.

[2] M.D. Barringer, O.T. Richard, J.P. Walter, S.M. Stitzel, K.A. Thole, Flow Field Simulations of a Gas Turbine Combustor, Journal of Turbomachinery 124 (2002) 508-516.

[3] W.F. Colban, A.T. Lethander, K.A. Thole, G. Zess, Combustor turbine interface studies-Part 2: Flow and thermal field measurements, Journal of Turbomachinery 125 (2003) 203-209.

[4] E. Kianpour, N.A. Che Sidik, M. Agha Seyyed Mirza Bozorg, Thermodynamic analysis of flow field at the end of combustor simulator, International Journal of Heat and Mass Transfer 61 (2013) 389.

[5] E. Kianpour, C. S. Nor Azwadi, M. Agha Seyyed Mirza Bozorg. 2012. Jurnal Teknologi. 58: 5.

[6] S. Patil, S. Abraham, D. Tafti, S. Ekkad, Y. Kim, P. Dutta, H. Moon, R. Srinivasan, Experimental and numerical investigation of convective heat transfer in a gas turbine can combustor, Journal of Turbomachinery 133 (2011) 1-8.

[7] G. Scheepers, R.M. Morris, Experimental study of heat transfer augmentation near the entrance to a film cooling hole in a turbine blade cooling passage, Journal of Turbomachinery 131 (2009) 044501.

[8] N. Sundaram, K.A. Thole, Bump and trench modifications to film-cooling holes at the vane-endwall junction, Journal of Turbomachinery 130 (2008) 041013.

[9] S. Baheri, S.A. Tabrizi, B.A. Jubran, Film cooling effectiveness from trenched shaped and compound holes, Heat and Mass Transfer 44 (2008) 989-998.

[10] S.A. Lawson, K.A. Thole, simulations of multiphase particle deposition on endwall film-cooling, Journal of Turbomachinery, 134 (2012) 011003.

[11] Y. Lu, A. Dhungel, S.V. Ekkad, R.S. Bunker, Effect of trench width and depth on film cooling from cylindrical holes embedded in trenches, Journal of Turbomachinery 131 (2009) 011003.

[12] J. Maikell, D. Bogard, J. Piggush, A. Kohli, experimental simulation of a film cooled turbine blade leading edge including thermal barrier coating effects, Journal of Turbomachinery 133 (2011) 011014.

[13] G. Barigozzi, G. Franchini, A. Perdichizzi, S. Ravelli, Effects of trenched holes on film cooling of a contoured endwall nozzle vane, Journal of Turbomachinery 134 (2012) 041009.

[14] R.P. Somawardhana, D.G. Bogard, Effects of obstructions and surface roughness on film cooling effectiveness with and without a transverse trench, Journal of Turbomachinery 131 (2009) 011010.

[15] K.L. Harrison, J.R. Dorrington, J.E. Dees, D.G. Bogard, R.S. Bunker, Turbine airfoil net heat flux reduction with cylindrical holes embedded in a transverse trench, Journal of Turbomachinery 131 (2009) 011012.

[16] C. Shuping, PhD thesis, University of Pittsburgh, Pittsburgh, PA, USA, 2008.

[17] S.B. Islami, B.A. Jubran, The effect of turbulence intensity on film cooling of gas turbine blade from trenched shaped holes, Heat and Mass Transfer 48 (2012) 831-840.

[18] Y. Lu, S. V. Ekkad. 2006. in Proceedings of the 9th AIAA/ASME Joint hermophysics and Heat Transfer Conference Proceedings.

[19] W. Ai, R.G. Laycock, D.S. Rappleye, T.H. Fletcher, J.P. Bons, Effect of particle size and trench configuration on deposition from fine coal fly ash near film cooling holes, Energy & Fuels 25 (2011) 1066-1076.

[20] W. Colban, K.A. Thole, M. Haendler, A comparison of cylindrical and fan-shaped film-cooling holes on a vane endwall at low and high freestream turbulence levels, Journal of Turbomachinery 130 (2008) 031007.

[21] W. Colban, A. Gratton, K.A. Thole, M. Haendler, Heat transfer and film-cooling measurements on a stator vane with fan-shaped cooling holes, Journal of Turbomachinery 128 (2006) 53-61.

[22] W. Peng, P. X. Jiang. 2012. Experimental Heat Transfer. 25(4): 282.

[23] E. Lutum, J. Von Wolfersdorf, K. Semmler, S. Naik, B. Weigand. 2002. Heat and Mass Transfer. 38(1): 7.

[24] Z. Gao, D. Narzary, J.C. Han, Turbine blade platform film cooling with typical stator-rotor purge flow and discrete-hole film cooling, Journal of Turbomachinery 131 (2009) 041004.

[25] S. Stitzel, K.A. Thole, Flow field computations of combustor-turbine interactions relevant to a gas turbine engine, Journal of turbomachinery 126 (2004) 122-129.